Int. J. Electrochem. Sci., 14 **(2019)** 3644 – 3650, doi: 10.20964/2019.04.28

International Journal of
ELECTROCHEMICAL
SCIENCE
www.electrochemsci.org

Short Communication

Preparation and Electrochemical Performance of Various Morphologies Cobalt Oxide as Anode Materials for Lithium-ion Batteries

Yongjun Wu[1,2,*], *Jing Han*[1], *Nina Xie*[3]

[1] Maanshan Teacher's College, Maanshan 243041, PR China
[2] College of Chemistry and Materials Science, Anhui Key Laboratory of Functional Molecular Solids, Anhui Normal University, Wuhu 241000, PR China
[3] Maanshan Ninth Junior High School, Maanshan 243000, PR China
[*]E-mail: wyj@massz.edu.cn

Received: 6 December 2018 / *Accepted:* 21 January 2019 / *Published:* 10 March 2019

Morphology controlled cobalt oxides are successfully prepared via hydrothermal reaction by monitoring the hydrothermal time. After that, the two different morphologies of cobalt oxide (CO-100, CO-130) are used as anode materials for lithium-ion batteries. The SEM and TEM images show that the CO-100 exhibits hollow sphere structure, while the CO-130 displays layered hollow sphere structure. The electrochemical results indicate that the CO-130 has more excellent cycle stability and capacity value than the CO-100. This phenomenon is ascribed to the novel structure of as-prepared CO-130, which could provide sufficient space for the electrolyte storage and wetting.

Keywords: Hollow sphere; Cobalt oxide; Capacity; Electrochemical performance

1. INTRODUCTION

Cobalt oxide has normal spinel structure, CO^{3+} occupies octahedral position, has high crystal field stabilization energy, and is very stable in air below 800℃ [1]. It is an excellent catalyst material. Co_3O_4 powder is widely used in catalysts, pigments, glazes, colored glasses, magnetic materials, cemented carbides and other fields, especially in the manufacture of thermal and piezoelectric electrodes, color TV glass shells and high-grade blue and white ceramics [2, 3, 4]. In addition to the chemical properties of the materials themselves, the application effect of Co_3O_4 in these areas is also related to the special effects of its fineness. Therefore, the synthesis of high quality Co_3O_4 powders has an important application value [5, 6].

Cobalt oxides can be obtained via heating and decomposition of precursors in sexual

atmosphere or air. Their advantages are that the morphology and particle size of the particles are easy to control, low cost and perfect dispersion. Moreover, the industrialization is easy, and the prospect is broad [7, 8]. However, the synthesis of the required precursors is still a subject worthy for further study [9]. In addition, hydrothermal synthesis is a wet chemical method for material preparation and research, which has been widely used in the fields of single crystal, thin film and powder preparation [10, 11]. Hydrothermal synthesis has the advantages of mild reaction conditions, high purity, small particle size and uniform distribution, no agglomeration, good dispersion and controllable morphology [12].

In this work, morphology controlled cobalt oxides are successfully prepared via hydrothermal reaction by monitoring the hydrothermal time. After that, the two different morphologies of cobalt oxide (CO-100, CO-130) are used as anode materials for lithium-ion batteries. The SEM and TEM images show that the CO-100 exhibits hollow sphere structure, while the CO-130 displays layered hollow sphere structure. The electrochemical results indicate that the CO-130 has more excellent cycle stability and capacity value than the CO-100. This phenomenon is ascribed to the novel structure of as-prepared CO-130, which could provide sufficient space for the electrolyte storage and wetting.

2. EXPERIMENTAL

2.1. Preparation of CO-100 and CO-130

Typically, 1.2 g $Co(NO_3)_2$ $6H_2O$ and 0.3 g $Co(NH_2)_2$ are added into 60 ml de-ionized water under stirring until all solid materials are dissolved into the water. After that, the mixed solution is transferred into autoclave at 100℃ and 130℃ for 24 h, respectively. Finally, the obtained sample is heated at 350℃ for 2 h to prepare Co_3O_4. The as-prepared samples are denoted as CO-100, CO-130, respectively.

2.2. Materials Characterizations

The structure of all samples were characterized by scanning electron microscopy (SEM, Ultra55) and transmission electron microscopy (TEM, FEI Tecnai G2 F20), an X-ray diffractometer (XRD, D8 Advance, BRUKER). X-ray photoelectron spectroscopy (XPS) measurements were conducted on XPS-7000 spectrometer.

2.3. Electrochemical Measurements

The working electrode was prepared by coating the slurry of the active material (20 mg), carbon black (2.5 mg), and 60 wt% polytetrafluoroethylene (1.6 mL) in a small amount of NMP on Cu film. Subsequently, the electrodes were dried at 110℃ for 24 h. Electrochemical measurements were conducted on an electrochemical working station (CHI 760E). All electrochemical behaviors of the working electrodes were cyclic voltammetry, galvanostatic charge-discharge and cycling stability.

3. RESULTS AND DISCUSSIONS

Figure 1 shows the SEM and TEM images of the as-prepared CO-100 and CO-130. As shown in Figure 1a and b, the CO-100 shows sphere structure. And the surface of CO-100 is smooth. However, the surface of CO-130 is consisted of layered structure. In all, the morphology of CO-130 is nano-sphere structure. To further confirm the interal structure of CO-100 and CO-130, TEM test was applied. As shown in Figure 1c and d, the CO-100 and CO-130 display hollow sphere structure [13]. The dimeter of CO-100 and CO-130 are located at 50~60 nm. As we all know, the performance of material mainly depends on the structure of the as-prepared materials. Because of the presence of hollow sphere structure, the CO-130 provides sufficient space for the electrolyte storage and wetting.

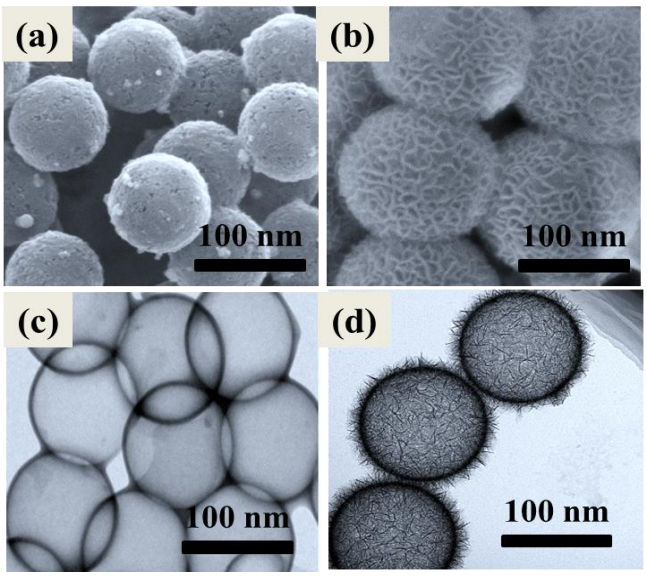

Figure 1. SEM images of (a) CO-100, (b) CO-130. TEM images of (c) CO-100, (d) CO-130.

The XRD test was conducted to determine the purity of the as-prepared CO-100 and CO-130. As shown in Figure 2a, the CO-100 and CO-130 show the same XRD pattern, indicating the successfully preparation of CO. Besides, all diffraction peaks are well matched with the standard card of CO [14, 15]. These results confirm the high crystal of the as-prepared various morphologies of Co_3O_4 anode materials. Besides, it can be concluded that the CO-100 and CO-130 have the same crystal structure. Figure 2b is the XPS of the CO sample. The XPS result can demonstrate the valence of the elements in the materials. As it can be seen that from the Figure 2b, the peaks at 780.2 ev and 795.3 ev are ascribed to the 2p of Co. This result clearly indicates that the CO samples are prepared successfully.

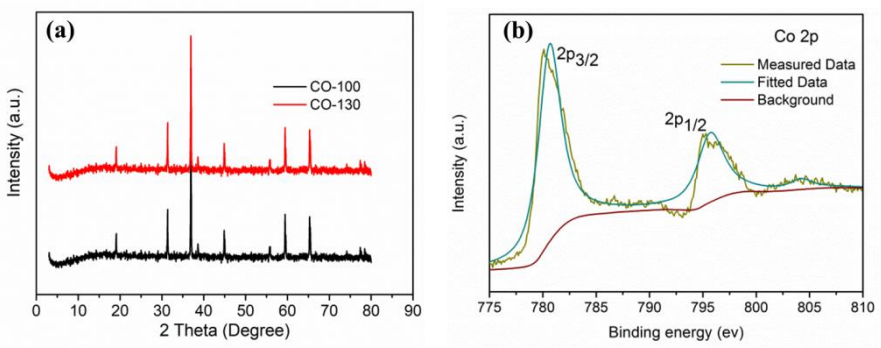

Figure 2. (a) XRD pattern of CO-100 and CO-130. (b) XPS of the as-prepared CO sample.

Figure 3a demonstrates the charging-discharging curves of the CO-100 and CO-130. All curves have the characteristics of typical CO charging and discharging platforms. First, there is an obvious discharge platform at about 1.25 V. The first discharge capacity of CO-130 is 1306 mAh g^{-1}, which is higher than the CO-100 (1286 mAh g^{-1}). Moreover, the coulombic efficiency of the CO-130 is about 89.6%. However, the CO-100 is only 85.2%. Figure 3b displays the CV curves of CO-100 and CO-130. As it can be seen from the figure, a large cathodic peak at 0.53 V is observed in the first cycle [16, 17]. This is corresponding to the lithium intercalation reduction peak of CO. In a word, the superior electrochemical performance is ascribed to the novel structure of as-prepared CO-130, which could provide sufficient space for the electrolyte storage and wetting.

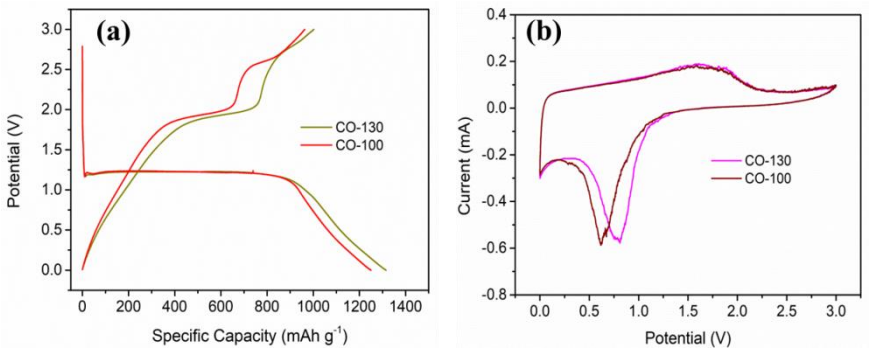

Figure 3. (a) Discharge-charge profiles of CO-100 and CO-130. (b) CV curves of CO-100 and CO-130.

Figure 4a shows the cycle performance of the CO-100 and CO-130. After 100 cycles, the specific capacity of CO-130 remains at 1008 mAh g^{-1} with a capacity retention of 86%, demonstrating excellent cycle stability. As for the CO-100, the specific capacity is only 802 mAh g^{-1} with the capacity retention of 68% [18]. To further indicate the excellent electrochemical performance of CO-130, the comparison of rate performance between CO-100 and CO-130 is conducted. As shown in Figure 4b, it can be observed that the CO-130 could endure the changes of current densities from 0.05 C to 2 C [19, 20]. Even at high current density of 2 C, the specific capacity of CO-130 is 1136 mAh g^{-1}. However, the CO-100 shows severe capacity fading when the current densities are improved from 0.05 C to 2 C [21].

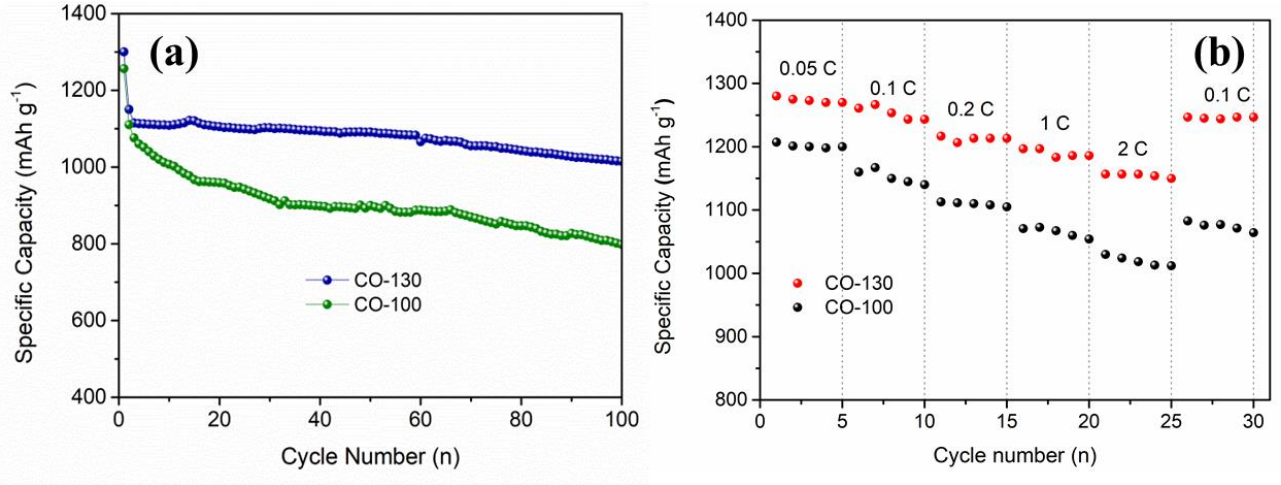

Figure 4. (a) The cycle stability of CO-100 and CO-130. (b) Rate performance of CO-100 and CO-130 at kinds of current densities.

Table 1 lists the electrochemical performance of various kinds of anode materials. As it can be seen that the as-prepared CO-130 material shows excellent cycle stability among various anode materials reported in the literature. It remains high capacity value of 1008 mAh g-1 after 100 cycles at the current density of 0.1 C. While the capacity values of other anode materials fade rapidly after 100 cycles. This improved electrochemical performance is mainly due to the hollow sphere structure of CO-130, which provides efficient space for the storage of electrolyte.

Table 1 The electrochemical performance of various anode materials for lithium-ion batteries.

Sample	Current Density	Cycle Number	Specific Capacity	Reference
CO-GN	0.1 C	50	1036 mAh g^{-1}	24
CO-MOF	0.1 C	100	810 mAh g^{-1}	25
P-CO-NT	0.1 C	60	856 mAh g^{-1}	26
Co_3O_4 tubular	0.1 C	100	727 mAh g^{-1}	27
CO-130	0.1 C	100	1008 mAh g^{-1}	This Work

4. CONCLUSIONS

In summary, morphology controlled cobalt oxides are successfully prepared via hydrothermal reaction by monitoring the hydrothermal time. After that, the two different morphologies of cobalt oxide (CO-100, CO-130) are used as anode materials for lithium-ion batteries. Among these two samples, the CO-130 shows excellent cycle stability and superior rate performance. This improved performance is ascribed to the novel structure of as-prepared CO-130, which could provide sufficient

space for the electrolyte wetting. In all, our work may provide a promising method for preparing high performance anode materials for lithium-ion batteries.

ACKNOWLEDGEMENT
This work is supported by the Key Natural Science Research Project of Anhui Province (KJ2014A246), the Key Teaching Research Project of Anhui Province (2015jyxm458), and the Quality Engineering Project of Anhui Province High level teaching team (2018jxtd058).

References

1. Y. Jiang, X. M. Yan, P. Mei and H. L. Tang, *J. Alloy Compd.,* 764 (2018) 80.
2. G. R. Wang, F. L. Zhu, J. Xia, L. Wang, Y. S. Meng and Y. Zhang, *Electrochim. Acta*, 257 (2017) 138.
3. L. W. Ye, Y. F. Yuan, D. Zhang, M. Zhu, S. M. Yin, Y. B. Chen and S. Y. Guo, *Mater. Lett*., 232 (2018) 228.
4. D. Q. Xin, J. F. Dai, J. F. Liu, Q. Wang and W. X. Li, *Mater. Lett*., 209 (2017) 388.
5. Y. L. Zhang, Y. Li, J. Chen, P. P. Zhao, D. G. Li, J. C. Mu and L. P. Zhang, *J. Alloy Compd*., 699 (2017) 672.
6. G. Z. Liu, X. G. Yuan, Y. M. Yang, J. M. Tao, Y. B. Chi, L. X. Hong, Z. Y. Lin, Y. B. Lin and Z. G. Huang, *J. Alloy Compd*., 780 (2019) 948.
7. Y. Y. Chen, Y. Wang, H. X. Yang, H. Gan, X. W. Cai, X. M. Guo, B. Xu, M. F. Lv and A. H. Yuan, *Ceram. Int*., 43 (2017) 9945.
8. M. M. Liang, M. S. Zhao, H. Y. Wang, F. Wang and X. P. Song, *J. Energ. Storage*, 17 (2018) 311.
9. F. X. Wang, Q. G. Han, Z. Yi, D. Geng, X. Li, Z. Wang and L. M. Wang, *J. Electroanal. Chem*., 807 (2017) 196.
10. H. M. Liang, Z. X. Wang, H. J. Guo and X. H. Li, *Ceram. Int*., 43 (2017) 11058.
11. B. Wang, X. Y. Lu, C. W. Tsang, Y. H. Wang, W. K. Au, H. F. Guo and Y. Y. Tang, *Chem. Eng. J*., 338 (2018) 278.
12. T. F. Yi, P. P. Peng, X. Han, Y. R. Zhu and S. H. Luo, *Solid State Ionics*, 329 (2019) 131.
13. Y. Jiang, X. M. Yan, P. Mei, Y. Zhang, W. Xiao and H. L. Tang, *J. Alloy Compd*., 764 (2018) 80.
14. B. N. An, Q. Ru, S. J. Hu, X. Song and J. Li, *Mater. Res. Bull*., 60 (2014) 640.
15. D. Y. Zhao, Q. Hao and C. X. Xu, *Electrochim. Acta*, 211 (2016) 83.
16. X. Q. Niu, X. L. Wang, D. Xie, D. H. Wang, Y. D. Zhang, Y. Li, T. Yu and J. P. Tu, *ACS Appl. Mater. Inter*., 7 (2015) 16715.
17. Y. Lu, S. L. Shi, F. Yang, T. Y. Zhang, H. Y. Niu, T. Wang, *J. Alloy compd*., 767 (2018) 23.
18. L. M. Jin, F. He, W. L. Cai, J. X. Huang, B. H. Liu and Z. P. Li, *J. Power Sources*, 328 (2016) 536.
19. L. M. Yang, Z. L. Chen, D. Cui, X. B. Luo, B. Liang, L. X. Yang, T. Liu, A. J. Wang and S. L. Luo, *Chem. Eng. J*., 359 (2019) 894.
20. P. H. Shao, J. Y. Tian, F. Yang, X. G. Duan, S. S. Gao, W. X. Shi, X. B. Luo, F. Y. Cui, S. L. Luo and S. B. Wang, *Adv.Funct. Mater*., 28 (2018) 1705295.
21. N. Li, S. F. Tang, Y. D. Rao, J. B. Qi, P. K. Wang, Y. Jiang, H. M. Huang, J. M. Gu and D. L. Yuan. *Electrochim. Acta,* 270 (2018) 330.
22. X. B. Luo, C. C. Wang, L. C. Wang, F. Deng, S. L. Luo, X. M. Tu and C. T. Au, *Chem. Eng. J*., 220 (2013) 98.
23. Q. Sun, Y. Yang, Z. Zhao, Q. Zhang, X. Zhao, G. Nie, T. Jiao and Q. Peng, *Environ. Sci: Nano,*10 (2018) 2440.

24. Q. M. Su, W. W. Yuan, L. B. Yao, Y. S. Wu, J. Zhang and G. H. Du, *Mater. Res. Bull*., 72 (2015) 43.
25. Y. Wang, B. F. Wang, F. Xiao, Z. G. Huang, Y. J. Wang, C. Richardson, Z. X. Chen, L. F. Jiao and H. T. Yuan, *J. Power Sources*, 298 (2015) 203.
26. M. H. Chen, X. H. Xia, J. H. Yin and Q. G. Chen, *Electrochim. Acta*, 160 (2015) 15.
27. X. Zhang, Z. Yang, C. Li, A. J. Xie and Y. H. Shen, *Appl. Surf. Sci*., 403 (2017) 294.